

Measurement and characterization of mixed mode fracture in concrete

J.S. Jacobsen, P.N. Poulsen & J.F. Olesen
Technical University of Denmark

ABSTRACT: The Mixed Mode fracture behavior of concrete is measured and characterized by investigating a single crack in a double-notched specimen. To obtain the characterization a very stiff biaxial test set-up with a closed loop control is constructed. The opening and sliding components of the Mixed Mode displacement are measured using a specially designed orthogonal gauge, and the measurements are used directly as the closed loop control signals. The closed loop control leads to an accurate and precise control and determination of the Mixed Mode phenomenon. A high-resolution Digital Image Correlation system, which is used for the determination of the displacement field in the close vicinity of the crack, supports the directly measured Mixed Mode behavior. Results are reported for a range of Mixed Mode angles.

1 INTRODUCTION

Experimental results directly describing the Mixed Mode fracture behavior in concrete are an essential basis for establishing a reliable constitutive material model for Mixed Mode fracture in concrete. In Mode I both adequate results and models are already established and several models for Mixed Mode have been suggested. Also Mixed Mode experimental results have been reported but with some uncertainties regarding the set-up and results, which lead to an indirect crack determination. The present paper outlines a method for the determination and characterization of Mixed Mode behavior of cracks in concrete.

In order to capture the direct material behavior of Mixed Mode fracture, a biaxial testing machine, which is capable of imposing both normal and shear loads on a given crack area, is needed. Previously Three significant biaxial set-ups have been presented by Hassanzadeh (1992), Nooru-Muhamed (1992) & Østergaard et al. (2007), respectively. Nooru-Muhamed (1992) developed a setup in which three frames were used to induce the mixed mode loading condition. Hassanzadeh (1992) developed a set-up suited for mounting in a standard testing machine, and with a separate second axis the mixed mode loading condition was established. Østergaard et al. (2007) developed a biaxial set-up consisting of a stiff support structure and a separate second axis. The Mixed Mode loading condition is established by mounting both the support structure and the second axis in a standard testing machine.

The stiffness of the two first mentioned set-ups is not documented, and for Hassanzadeh (1992) there are humps on the descending branch, which normally are associated with insufficient stiffness, see e.g. Hillerborg (1989). Crack patterns reported by Nooru-

Muhamed (1992) consist of shear cracks, which can only lead to an indirect determination of the Mixed Mode behavior. In the set-up by Østergaard et al. (2007) the double-notched specimen had a side length of 150 mm and depth of 100 mm. The relatively high specimen introduced a large amount of elastic energy in the set-up. The larger elastic energy made the fracture initiation unstable and extremely difficult to control. Therefore according to the stiffness considerations, the specimen dimensions were reduced by Petersen (2008). Petersen (2008) tested specimens with the dimensions $150 \times 80 \times 75 \text{ mm}^3$ and notch depth of 37.5 mm, see Figure 1. The significant lower height reduced the amount of elastic energy. Both Østergaard et al. (2007) & Petersen (2008) used the piston displacements as the control signal. According to Petersen (2008) this resulted in a large deviation between the prescribed Mixed Mode angle, i.e. the ratio between opening and sliding, and the actual angle achieved. The large deviation made it difficult to control the test and made an inverse analysis of the test results necessary.

In the present set-up, which is an enhancement of the set-up by Østergaard et al. (2007), the control is changed such that the vertical and the horizontal axis can be controlled independently in a closed control loop. Referring to Gettu et al. (1996), a more stable and robust fracture control is obtained by using the actual opening and sliding over the ligament in the control. The measurements of the opening and sliding are obtained by using a specially designed gauge rail mounted on the specimen.

For small initial openings followed by a Mixed Mode loading, the specimen dimensions by Petersen (2008) clearly result in structural like response with either a curved crack path, as in Figure 1, or shear cracks as the primary fracture. By sawing the notches deeper to the present depth of 55 mm, each test results in a

single, primary crack between the two notches and few secondary shear cracks. Further, the deeper notch reduces the structural effects and results in a plane crack pattern, leading to a more direct material interpretation. Altogether the present set-up gives reliable material tests for a direct characterization of Mixed Mode fracture in concrete.

The following section presents the test set-up, the specimen, the orthogonal gauge rails used for mounting the clip gauges in a close vicinity of the crack and the test procedure. Finally, characteristic results from Mixed Mode tests, displaying relevant Mixed Mode ratios between opening and sliding for a single crack, are presented and analyzed.

2 TEST SET-UP

2.1 Testing Machine

A testing machine, which can apply simultaneous but independent normal and shear loads to a concrete specimen, has been constructed. The machine is intended for the investigation of the Mixed Mode fracture in concrete. Figure 2 shows the overall structure of the machine, which in a slightly different configuration was presented by Østergaard et al. (2007). The machine consists of two independent actuators and is controlled by a multi-axial Instron 8800 control unit. A four column Instron 5MN universal testing machine is the basis of the set-up, giving a very stiff and full functional vertical axis of loading. The horizontal axis is designed especially for the set-up and built into a very stiff support structure, such that the shear load is carried from the actuator through the specimen and back to the actuator through compression in the support structure. Thereby this custom made bi-axial hydraulic testing machine has a considerable rotational stiffness. In the bi-axial mode the vertical axis has a capacity of 100 kN, while the horizontal has a capacity of 50 kN.

The motions of the test specimen are conducted through two slides, a horizontal and a vertical. The slides, which can be seen in Figure 3, are constructed from low friction and high precision THK linear motion systems with oversized balls in the closed ball bearings. All bolted connections in the set-up are pre-stressed such that no slip between the steel plates can occur during the experiment. The specimen is glued into the set-up using sandblasted steel blocks, avoiding that stresses arise in the specimen during the attachment process.

2.2 Test Specimen

In Figure 3 the test specimen is shown in place in the testing machine. The test specimen is double-notched and has a width of 150 mm, a height of 80 mm and a depth of 75 mm. The notches are cut from the side and have a depth of 55 mm. Thereby the ligament area is $40 \times 75 \text{ mm}^2$. The specimens are cut

from a beam with a cross section of $150 \times 150 \text{ mm}^2$ and a length of 600 mm, and cast from a concrete with maximum aggregate size of 8 mm and a predicted 28 days strength of 30 MPa. The deeper notches should ensure that a single, relatively plane crack develops between the two notches, ensuring that results can be considered as material information.

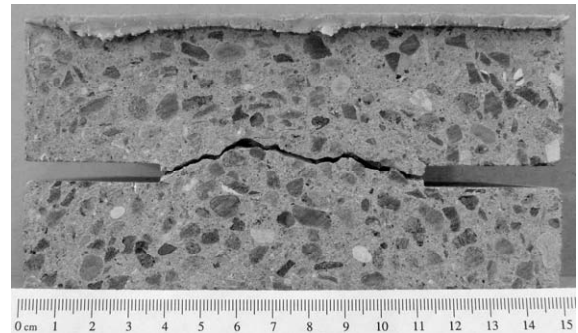


Figure 1. Test specimen in the configuration with short notches. Curved crack path between notches.

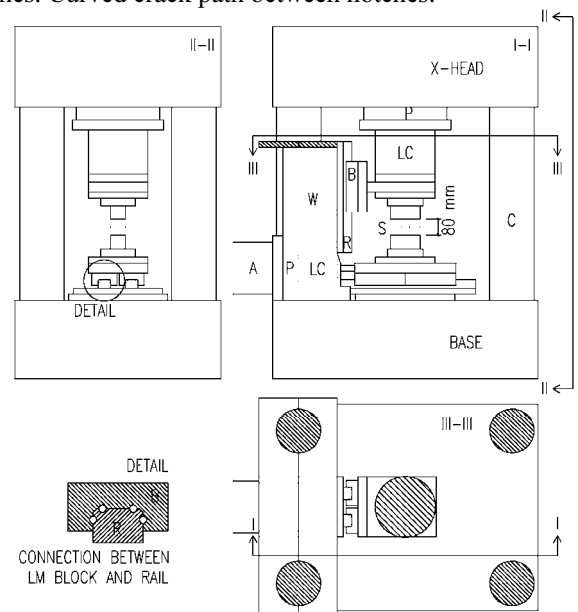


Figure 2. Sketch of biaxial set-up. A = actuator, P = piston, LC = load cell, S = specimen, C = column, B = linear motion block (LM block), R = Rail, W = web. Some background details are left out for clarity.



Figure 3. Test set-up showing a glued in test specimen, vertical load cell, support structure and the slides in both vertical and horizontal direction.

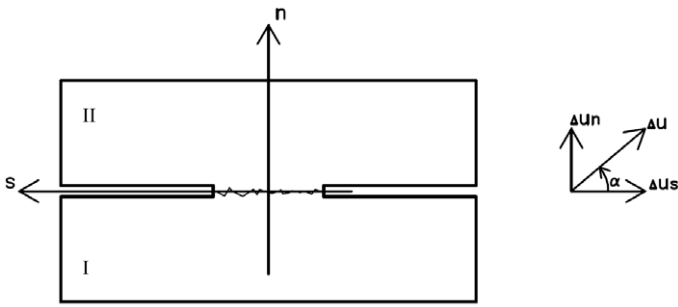


Figure 4. Local (n,s)-coordinate system and direction of positive relative displacements between the two specimen parts, I and II .

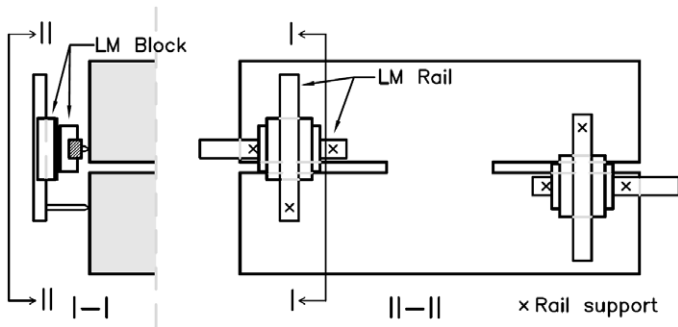


Figure 5. Principle sketch of gauges rails with Linear Motion (LM) rails, LM blocks and indication of rail supports.

2.3 Gauge Rails

A local (n,s)-coordinate system is introduced according to Figure 4. Fracture in the ligament divides the specimen in two parts, I and II , respectively. Relative displacements between the two parts, Δu_n and Δu_s in the n and the negative s direction, respectively, are defined as

$$\begin{aligned} \Delta u_n &= u_n^{II} - u_n^I \\ \Delta u_s &= u_s^I - u_s^{II} \end{aligned} \quad (1)$$

In the test the relative displacement Δu is assumed to be the same size along the ligament. The relative displacements are measured by four Clip Gauges (CGs) mounted on the specimen using two specially designed orthogonal gauge rails placed across the two notches. In pair the CGs measure the deformation in vertical and horizontal direction, respectively. The CGs allow for independent control of the vertical and horizontal axis in a closed control loop using the mean signal in respective directions as the response signal.

Figure 5 shows the principle structure of the orthogonal gauge rails, and Figure 6 shows gauge rails and CGs in use. Two small, high precision THK miniature Type LM Guides, THK (2008), are used in each orthogonal gauge rail. Low friction oversized ball bearings together with the CGs allow for the determination of displacements smaller than $1 \mu\text{m}$. The rails are assembled orthogonally through the blocks top on top, and a specially designed house around the blocks together with modified end blocks

enables the attachment of CGs. At the front of the specimen the gauge rail has three supports, two at one side of the notch supporting the horizontal rail and one at the opposite side supporting the vertical rail. The two horizontal and the vertical supports can move independently, allowing for the measuring of the relative displacement in both directions between the two parts of the specimen. The gauge rail is kept in place by an aluminum arm around the specimen. At the back, the aluminum arm's point support is placed close to the elastic centre of the triangle defined by the three front supports.

As illustrated by Madsen (2009), who used a pair of CGs mounted directly on the specimen, the test set-up is fully capable of performing full uniaxial opening histories and cyclic loading histories on the presented concrete specimens. Further, with the gauge rails the following illustrates that the set-up enables stable closed loop controlled Mixed Mode testing.

2.4 Test Procedure

Initially a crack is introduced between the notches by a pure Mode I opening, $\Delta u_s = 0$, and the crack is opened to a specified crack opening measured by the CGs. After the initiation of the crack the specimen can be exposed to both Mode 1 and 2 opening introducing a Mixed Mode opening of the crack. The Mixed Mode opening angle, α in Figure 4, is defined as the angle between the horizontal plane and the relative displacement, i.e.

$$\tan(\alpha) = \frac{\Delta u_n}{\Delta u_s} \quad (2)$$

Displacement velocity is set such that the peak load corresponding to f_t is captured in around 60 s and the test in total is finished in around 600 s. Slow opening pace ensures a more stable crack initiation, while the total time is sought limited to 600 s in an attempt to limit the influence of viscoelastic effects.

2.5 Aramis

Along with the CG signals the displacements are recorded by the high-resolution digital image correlation system Aramis by GOM mbH, GOM (2005). The Aramis system is a 3D photometric equipment and uses digital stereo photographing and subsequent triangulation to determine 3D displacements on the observed surface of the specimen. The system enables determination of the displacement field in a close vicinity of the crack. The four megapixels picture is divided into small regions called facets, which typically consist of 15×15 pixels. During the analysis the movement and deformation of the facets is registered and assembled. This analysis gives a

displacement field of the surface, which e.g. can be post-processed into a strain field. Figure 8a – e show typical results from the Aramis system.



Figure 6. Close view of test specimen, gauges rails and clip gauges.

3 RESULTS

3.1 Load Opening Displacement

At first the test specimen is loaded in pure tension with respect to the ligament between the two notches. This Mode 1 loading initiates a crack between the notches and results in a characteristic opening-displacement response shown in Figure 7. The normal stress σ , defined as the measured normal load divided by the ligament area, is plotted as function of the opening displacement Δu_n for different test specimens. During the loading in the elastic domain, the different tests almost coincide, while their maximum points are scattered in an interval of 0.5 MPa. After the maximum point the same scatter interval continues during the fracture initiation. The scatter is most likely caused by the natural variation of concrete properties. In three of the four cases the test set-up is capable of catching the softening branch and in the last case, for an additional opening, the softening branch is recaptured. These opening curves prove the sufficient stiffness of the test set-up. Starting the Mixed Mode at an opening of $\Delta u_n = 0.025$ mm clearly results in a drop in the normal stress but also a larger scatter caused by the combined loading in Mixed Mode. Further it is shown that starting the Mixed Mode displacement at an opening of $\Delta u_n = 0.025$ mm corresponds to a load level of 30 – 40 % of f_t .

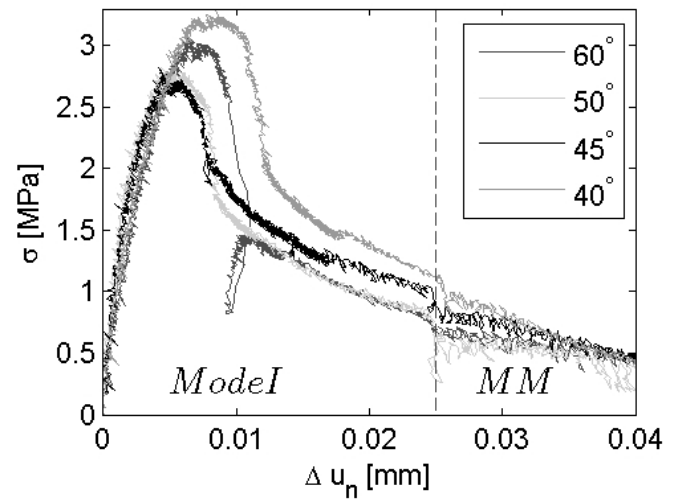


Figure 7. Initial load opening displacement curves for four different Mixed Mode angles. The dashed line indicates the start of Mixed Mode displacement (MM).

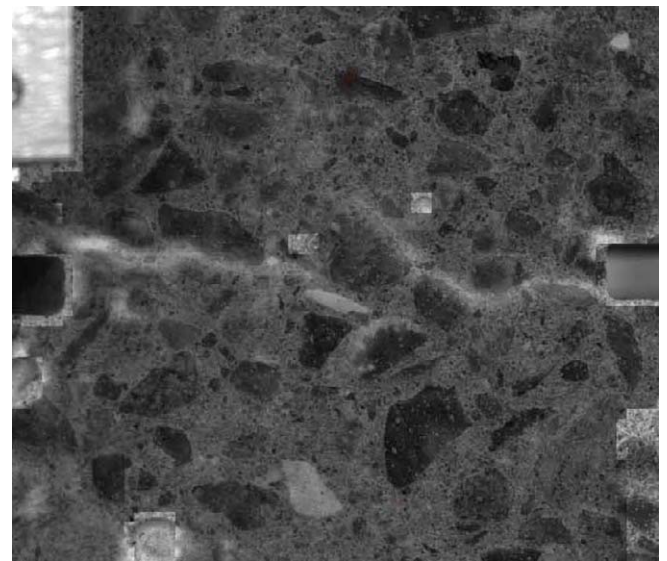


Figure 8a. Crack initiation for Mixed Mode angle of $\alpha = 50^\circ$. Maximum tension, crack not fully initiated.

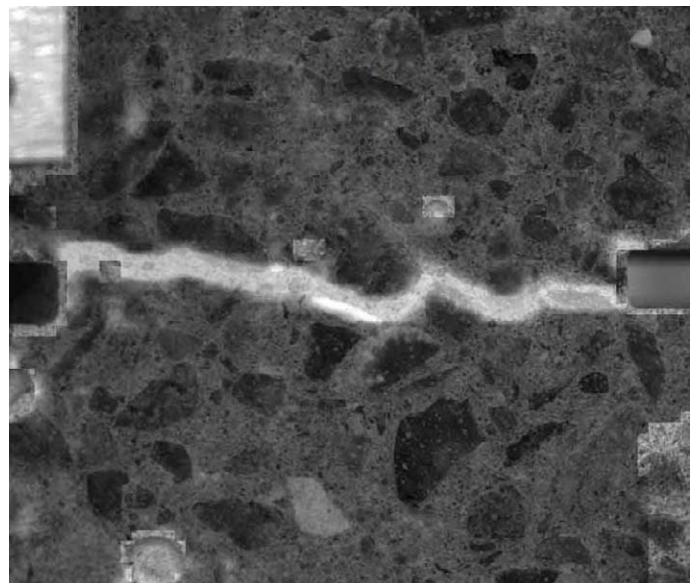


Figure 8b. Start Mixed Mode, crack fully localized.

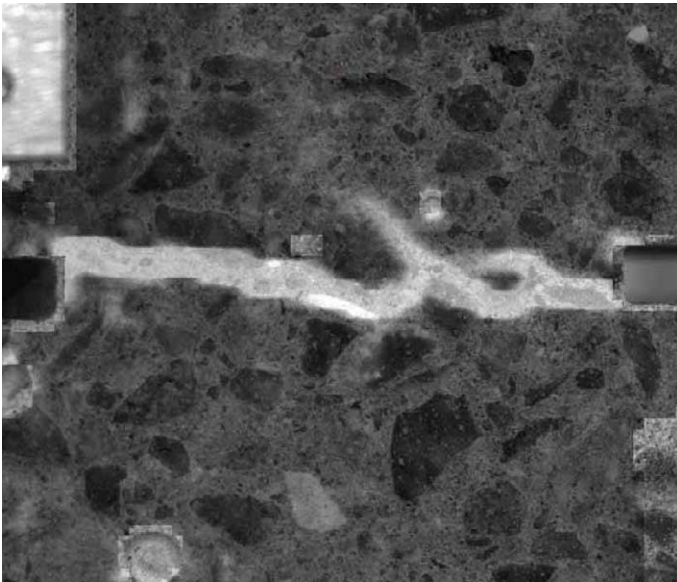


Figure 8c. Normal stress changing from tension to compression, initiation of secondary shear cracks.



Figure 8d. Maximum compression and shear. Propagating shear cracks and visible opening crack.

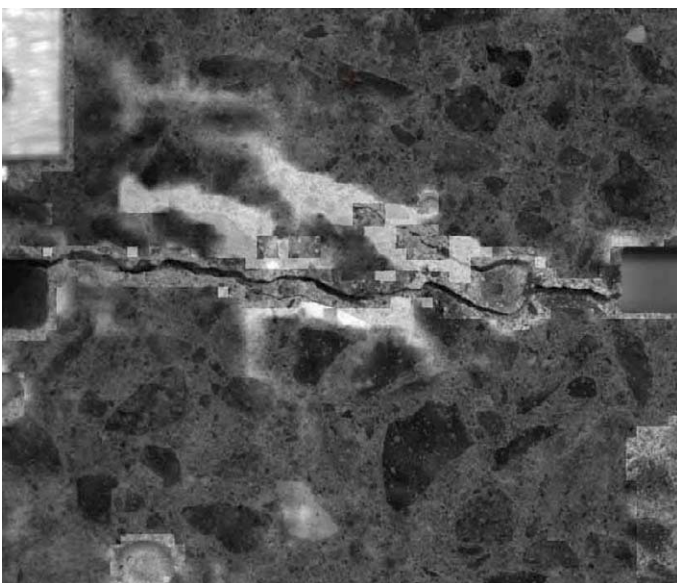


Figure 8e. Final crack pattern with clear primary crack and some shear fracture primary localized at the right notch.

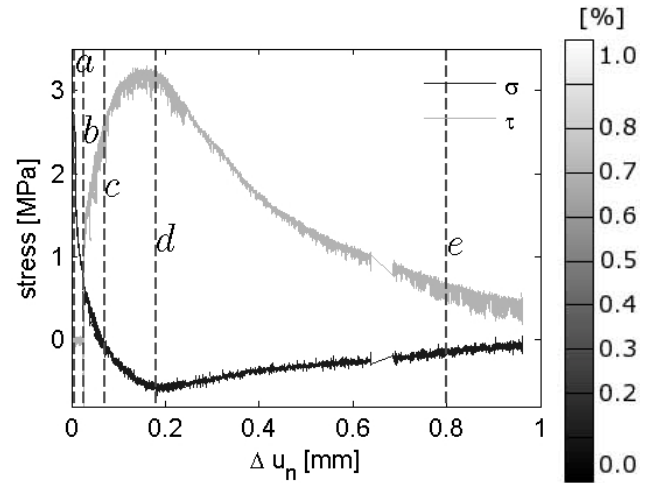


Figure 8f. Stress opening relation indicating test progress for the different Aramis pictures, Figure 8a – e. The data collection is divided in two series with a small time step in between which explains the jump in the measurements around $\Delta u_n = 0.7$. Strain scale for Aramis pictures made transparent, which make it possible to see the aggregate location.

3.2 Aramis Example

Using the photometric system Aramis, Figure 8 shows the fracture propagation during a Mixed Mode test. In the pictures the largest principal strain registered on the surface is shown. The definition of strain makes no sense in combination with localized cracking so the usage of strain is only for visualization purposes. After the crack initiation the specimen is displaced in a Mixed Mode angle of $\alpha = 50^\circ$, giving a bit more opening than shear. Figure 8f shows the normal stress σ and the shear stress τ plotted as functions of the opening displacement Δu_n . Stress stages for the matching pictures are indicated. σ and τ are defined as the measured normal and shear load divided by the ligament area, respectively.

The first picture, Figure 8a, shows the fracture development at peak load and clearly indicates that the crack localization between the notches is not fully established. Same observation is made by Petersen (2008) and by Østergaard et al. (2007), who state that a clear crack establishment is not obtained until the load has decreased by 20–50 % of the peak load. As shown in Figure 7, the load, at the beginning of Mixed Mode displacement, is reduced to 30–40 % of the peak load. At this displacement level clear crack localization is obtained, see Figure 8b. The test is displacement controlled, so after some Mixed Mode loading the dilational effects will shift the normal load from tension to compression. Figure 8c is snapped directly at this transition and despite a clear, primary crack some secondary shear cracks tend to grow. At maximum compression multiple secondary cracks have formed, see Figure 8d, but for the fracture propagation a clear primary crack between the two notches is still seen. The last picture, Figure 8e, shows the final fracture development for loads returning to zero, and a clear fracture area is

localized representing some secondary shear cracks and an apparent primary opening crack.

3.3 Mixed Mode Behavior

Figure 9 shows the Mixed Mode behavior for four specimens displaced at four different Mixed Mode angles from 40° to 60° dictated by the closed control loop. In Figure 9c the initial opening of $(\Delta u_n, \Delta u_s) = (0.025, 0)$ mm in each test is recognized and after the opening the combined opening, Δu_n , and sliding, Δu_s , is carried out. Deformations in Figure 9c are measured by the CG and are the actual responses to the demand almost without any noise. Figure 9d is the load opening displacement similar to Figure 8 but with interchanged axes and a considerable larger range of opening. Earlier in Figure 7 it has been shown that the tensile strength is located in an interval of 0.5 MPa, but here it is shown that the level of compression during the test rises for lowered Mixed Mode angle. Lowered Mixed Mode angle is equal to a higher level of sliding and thereby intensified dilational effects, which in the displacement controlled test results in more compression. Responses for 45° and 50° are roughly identical, which probably is an effect of the natural variation of concrete properties. The spike for 40° at maximum compression is caused by a change of fracture from a beginning shear crack away from the ligament to a more significant opening crack. Furthermore it is seen that

for 60° the level of compression is almost zero. Similar to Figure 9d for normal stress, the shear stress level, shown together with the shear displacement in Figure 9a, increase for lowered Mixed Mode angle where the sliding starts to dominate. Noise recognized on the different load-displacement curves is primarily caused by tuning difficulties with the closed loop control. Stiffness of the specimen changes remarkably during the test, which makes it difficult to find a single tuning level for the entire test, and some noise is expected. The noise reduction clearly seen on three of the four tests after the peak is caused by an increase in displacement rate, and thereby an indirect change in the tuning of the closed control loop signal. Figure 9b combines the results from the three other plots and shows the shear stress, τ , as function of the normal stress, σ . Despite the few tests there is a clear tendency in the Mixed Mode behavior, with almost straight lines in both loading and unloading before and after the peak in the stress-plot, respectively.

In the 40° test the relative large amount of sliding almost results in a shear fracture. The 60° test with a relatively large amount of opening is almost without any Mixed Mode effects. Overall the four tested Mixed Mode angles, for the chosen initial opening, cover the relevant test area from nearly encountering a shear fracture to an almost pure Mode I opening.

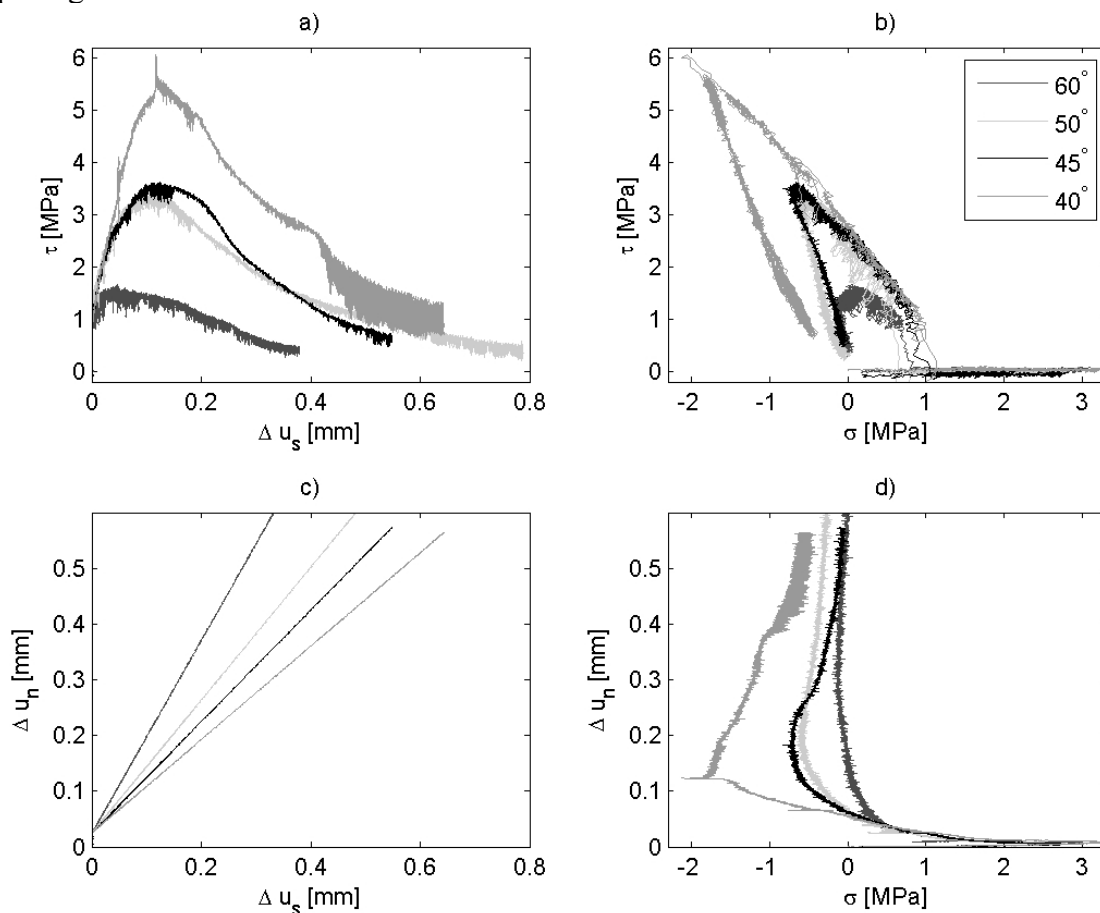


Figure 9. Mixed Mode test results for four different Mixed Mode angles.

4 CONCLUDING REMARKS

The biaxial test set-up with the new orthogonal gauge rails makes it possible to determine the relative opening and sliding over the ligament, and to use the relative displacements in the closed control loop. In Mode I, the set-up is sufficiently stiff and is, together with the closed control loop, capable of determining the fracture initiation. The orthogonal gauge rail results in a direct interpretation of the Mixed Mode fracture process, giving that the prescribed Mixed Mode angle is equal to the achieved response over the ligament.

Deeper notches on the specimen result in a more plane crack surface. As a result of the specimen design and the set-up design, the crack surface is more even and governed by material aspects like aggregate size and concrete strength rather than structural effects. Subsequent investigation of the total crack surface supports this interpretation. So, despite several shear cracks during the fracture development, the crack determination seems representative of a single crack in Mixed Mode loading.

The Mixed Mode tests show clear correlation between opening and sliding and related stresses, with higher shear stresses and more compression for lower angles. For the tested initial opening, the four Mixed Mode tests, with opening angles between 40° and 60° , cover the relevant range from nearly encountering a shear fracture to an almost pure Mode I opening.

REFERENCES

- Gettu, R., Mobacher, B., Carmona, S. & Jansen D.C. (1996). Testing of Concrete Under Closed-Loop Control. *Advanced Cement Based Materials* 3.2 (1996): pp. 54-71. Elsevier Science Inc.
- GOM (2005). Aramis User Manual (4M) v5.4.1. GOM mbH.
- Hassanzadeh, M. (1992). Behaviour of Fracture Process zones in Concrete Influenced by Simultaneously Applied Normal and Shear Displacements. PhD thesis, Report TVBM-1010, Lund Institute of Technology.
- Hillerborg, A. (1989). Stability problems in fracture mechanics testing. *Fracture of Concrete and Rock: Recent Developments*, pp. 369-378. Elsevier Applied Science.
- Madsen, A. (2009). Cracks in Concrete under Repetitive Load – Experiments and Modeling. Master Thesis, Department of Civil Engineering, Technical University of Denmark
- Nooru-Muhamed, M.B. (1992). Mixed Mode Fracture of Concrete: An Experimental Approach. PhD Thesis, Delft University.
- Østergaard, L., Olesen, J.F., & Poulsen, P.N. (2007). Biaxial testing machine for mixed mode cracking of concrete. *Fracture Mechanics of Concrete and Concrete Structures, New Trends in Fracture Mechanics of Concrete* (ISBN: 978-0-415-44065-3), Taylor & Francis/Balkema, The Netherlands, 263-270.
- Petersen, R.B. (2008). Fracture Mechanical Analysis of Reinforced Concrete. Master Thesis, Department of Civil Engineering, Technical University of Denmark, Project no. 07-062
- THK (2008). THK General Catalog. Catalog No. 400-1e.

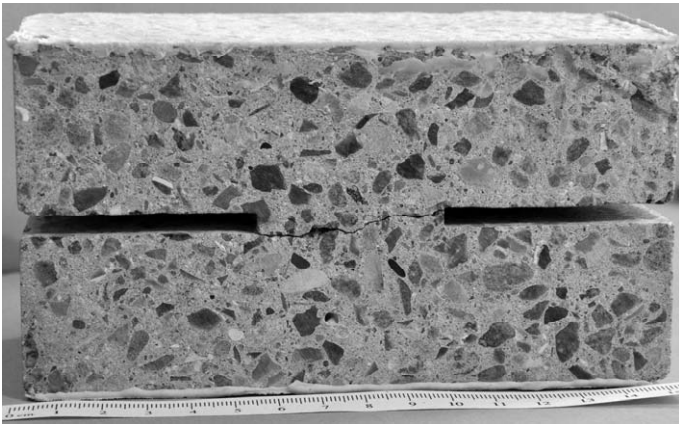


Figure 10. Final crack path for the 40° Mixed Mode test.

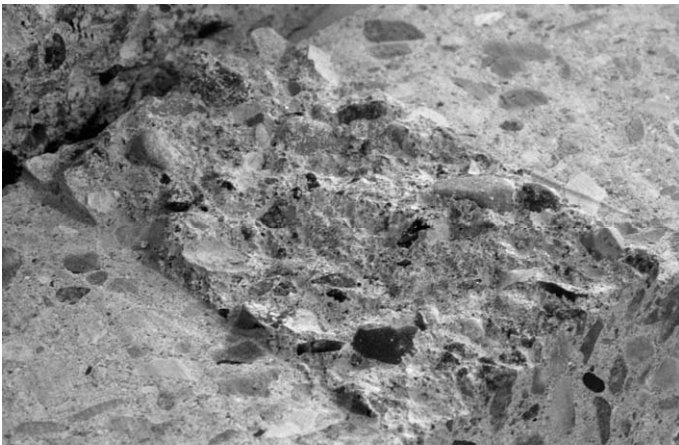


Figure 11. Close view of the crack surface for the 40° Mixed Mode test.

3.4 Crack Morphology

The test specimens are casted from a concrete with varying aggregate size up to 8 mm, and the concrete as a material is far from being homogenous. Therefore a completely straight crack path will not be possible. However, the crack path in the present tests is almost straight, with a variation smaller or equal to the notch height of 4 mm, see e.g. Figure 8e for 50° Mixed Mode and Figure 10 for 40° Mixed Mode. This fracture localization between the notches is a characteristic of the new test specimen, and structural effects obtained by the old test specimen by Petersen (2008), see Figure 1, are avoided by the new deeper notches. Having a closer view of the crack surface, see Figure 11 from the 40° Mixed Mode test, it is clear that the fracture is localized in between the aggregates, indicating the use of low strength concrete. Thereby the crack surface is influenced by the aggregate size but without the earlier reported structural effects. From all four tests the crack surface geometry seems only to depend on material properties like the aggregate size, and it seems reasonable to use the results in a material model.